Exp Astron (2009) 23:169–191
DOI 10.1007/s10686-008-9105-x

ORIGINAL ARTICLE

Stellar And Galactic Environment survey (SAGE)

M. A. Barstow · M. P. Kowalski · R. G. Cruddace · K. S. Wood · F. Auchere · N. J. Bannister · M. F. Bode · G. E. Bromage · M. R. Burleigh · A. C. Cameron · A. Cassatella · F. Delmotte · J. G. Doyle · B. Gaensicke · B. Gibson · C. S. Jeffery · C. Jordan · N. Kappelmann · R. Lallement · J. S. Lapington · D. de Martino · S. A. Matthews · M. Orio · E. Pace · I. Pagano · K. J. H. Phillips · M.-F. Ravet · J. H. M. M. Schmitt · B. Y. Welsh · K. Werner · G. Del Zanna

Received: 21 February 2008 / Accepted: 3 June 2008 / Published online: 15 August 2008

Abstract This paper describes a proposed high resolution soft X-ray and Extreme Ultraviolet spectroscopy mission to carry out a survey of Stellar and Galactic Environments (SAGE). The payload is based on novel diffraction grating technology which has already been proven in a sub-orbital space

M. A. Barstow (✉) · N. J. Bannister · M. R. Burleigh · J. S. Lapington
Department of Physics and Astronomy,
University of Leicester, Leicester, LE1 7RH, UK
e-mail: mab@star.le.ac.uk

M. P. Kowalski · R. G. Cruddace · K. S. Wood
Naval Research Laboratory, Code 7655, Washington, DC, USA

F. Auchere
Institut d'Astrophysique Spatiale, Université Paris Sud, Orsay, France

M. F. Bode
Astrophysics Research Institute, Liverpool John Moores University,
Birkenhead, CH411LD, UK

G. E. Bromage · B. Gibson
Centre for Astrophysics, University of Central Lancashire, Preston, PR1 2HE, UK

A. C. Cameron
School of Physics and Astronomy, University of St Andrews, Scotland, UK

A. Cassatella
Instituto Nazionale di Astrofisica, Universita Roma Tre, Rome, Italy

F. Delmotte · M.-F. Ravet
Institut d'Optique, Campus de Polytechnique, Palaiseau, France

J. G. Doyle · C. S. Jeffery
Armagh Observatory, Armagh, BT61 9DG, Northern Ireland, UK

mission and which is ready to fly on a satellite platform with minimal development. We discuss the goals of a SAGE base-line mission and demonstrate the scientific importance of high resolution spectroscopy in the Extreme Ultraviolet for the study of stars and the local interstellar medium.

Keywords Stars · White dwarfs · AGN · Cataclysmic variables · Extreme ultraviolet · Spectroscopy · Gratings · MCP detectors

1 Introduction

The formation and evolution of stars, their interaction with interstellar material and the ultimate effect of all the various physical processes on their planetary systems is still poorly understood. Crucial elements of the picture concern the levels of activity in main sequence stars and the resulting stellar winds

B. Gaensicke
Department of Physics, University of Warwick, Coventry, UK

C. Jordan
Department of Physics, University of Oxford, Oxford, UK

N. Kappelmann · K. Werner
Institut für Astronomie und Astrophysik, Universität Tübingen, Tübingen, Germany

R. Lallement
Service d'Aeronomie du CNRS, 91371, Verrières-le-Buisson, France

D. de Martino
INAF, Osservatorio Astronomico di Capodimonte, Napoli, Italy

S. A. Matthews · K. J. H. Phillips · G. Del Zanna
Solar and Stellar Physics, Mullard Space Science Laboratory,
Holmbury St Mary, Dorking, UK

M. Orio
INAF, Osservatorio Astronomico di Padova, Padova, Italy

E. Pace
Dip. Astronomia e Scienza dello Spazio, Universita Firenze, Florence, Italy

I. Pagano
INAF, Osservatorio Astrofisico di Catania, Catania, Italy

J. H. M. M. Schmitt
Hamburger Sternwarte, Universität Hamburg, Hamburg, Germany

B. Y. Welsh
Space Sciences Laboratory, University of California, Berkeley, CA, USA

which can directly affect planetary environments on a range of timescales. In addition, stellar winds control the flow of material and flux of cosmic rays from the galactic environment which also have a potential influence on climate. Ultimately, stars recycle material back into the interstellar medium, enriching galactic metal content, through the production of white dwarfs and supernovae. All the important processes involved in these stellar lifecycles are traced by the presence of hot (10^5–10^7 K) gas. Therefore, a high resolution soft X-ray and Extreme Ultraviolet (EUV) spectroscopy mission is needed to carry out a survey of Stellar and Galactic Environments (SAGE). SAGE will investigate the density, temperature, composition, structure, and dynamics of hot astrophysical plasmas in the 100,000 to 10 million degrees Kelvin range, addressing basic questions of stellar evolution and galactic structure. Key scientific goals will be to:

Examine the structure and dynamics of stellar coronae: to determine the origins and evolution of coronal activity over stellar lifetimes and the influence of this activity on astrospheres and the interstellar medium (ISM).

Study the evolution of white dwarfs: to examine the physical mechanisms controlling the atmospheric abundances and understand how important elements such as CNO are returned to enrich the interstellar medium; determine the incidence of circumstellar material associated with the disruption of remnant planetary systems.

Probe the structure and ionization of the local interstellar gas: measuring density, temperature, ionization state, and depletion level of gas clouds along many lines-of-sight within 200 pc of the Sun.

Study of accreting white dwarf binaries: to diagnose temperature, densities and composition of accretion flows and the physical status of accreting white dwarfs in cataclysmic variables and in super-soft x-ray sources.

The programme is relevant to aspects of all four of ESA's primary Cosmic Vision themes, but concentrates on particular sub-themes:

What are the conditions for planet formation and the emergence of life?

Life and habitability in the Solar System (effects of stellar activity on habitability)

How does the Solar System Work?

From the Sun to the edge of the Solar System (interaction of the heliosphere and ISM)

What are the fundamental physical laws of the Universe?

Matter under extreme conditions (degenerate matter, accretion onto compact objects)

How did the Universe originate and what is it made of?

The evolving violent Universe (lifecycles of matter and the galactic environment)

EUVE and the ROSAT WFC left a great legacy in astrophysics at EUV wavelengths. EUVE introduced EUV spectroscopy, and the X-ray observatory Chandra has demonstrated the promise of high-resolution spectroscopy with the Low Energy Transmission Grating (LETG). The termination of EUVE left a gap in spectral coverage at crucial EUV wavelengths. The NASA

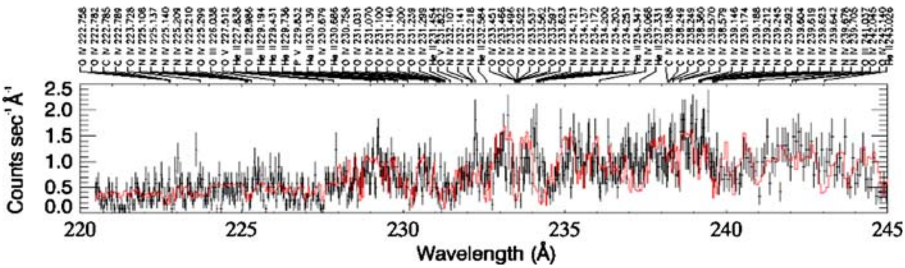

Fig. 1 High resolution spectrum of the white dwarf G191-B2B, obtained in a 300 s sounding rocket observation. The best-fit spectrum (red/grey histogram) yields a photospheric He abundance of 1×10^{-6} and LISM HeII column density of 5.9×10^{17} cm^{-2}

CHIPS mission has filled this gap only partially, as it is optimized for diffuse emission and has only moderate resolution.

The urgent need for a high resolution spectroscopic instrument has been thoroughly documented in a review of EUV astronomy [1] and in an AAS Meeting (Albuquerque 2002) Topical Session [2]. The technology that will be utilised by SAGE is the climax of more than 20 years of research on multilayer coatings and ion-etched diffraction gratings. A SAGE prototype, J-PEX, has been flown successfully on NASA sounding rocket 36.195 DG in 2001 and obtained the first high resolution EUV spectrum of any source other than the Sun, the white dwarf (WD) G191-B2B [3, 4] (Fig. 1), achieving its prime science goal of detecting ionized helium, which was found to be mostly interstellar in origin.

The J-PEX mission and the SAGE instrument concept were developed by Kowalski and colleagues at the Naval Research Laboratory (NRL) in the USA as part of an ongoing research program in the use of multilayer coated optics for remote sensing in astrophysics and other areas. Under the name of APEX, the concept was originally proposed to NASA as a SMEX mission and published by Kowalski et al. [5, 6]. The instrument is a suite of 8 near-normal incidence spectrometers, similar to J-PEX, optimized for EUV wavelengths (~90–275 Å) with simultaneous high resolving power (~10,000) and effective area (30–50 cm^2). This allows application of the range of plasma diagnostic techniques that has already been used successfully in solar research, from satellites such as SOHO and the recently launched Hinode. This mission will yield a capability of studying the dynamics of the integrated light from other stars at the level of detail available for the Sun. For cosmic sources, even the Chandra LETG has comparatively modest efficiency and spectral resolution. For example, at 124 Å SAGE will deliver an effective area 8 times that of the Chandra LETG and more than five times the spectral resolution. High-resolution spectroscopy of hot plasmas will allow unambiguous detection and measurement of weak emission lines and absorption features, and the study of source structure and dynamics through measurement of line profiles and Doppler shifts.

2 Scientific objectives

The overall science theme for SAGE is centred on the formation and evolution of stars, their interaction with interstellar material and the ultimate effect of all the various physical processes on their planetary systems. Planetary environments are strongly influenced by levels of activity in their host stars, through high energy radiation from flares and related events as well as the stellar winds. Stellar winds are believed to have a strong influence on incident cosmic ray fluxes [7] and define the astropause, the boundary between the influence of the star and the surrounding ISM (analogous to the Heliopause for the Sun). Variations in the cosmic ray flux may have an influence on planetary climate [8]. Stellar winds are also a route for the flow of material into the interstellar environment. In particular, stars recycle material back into the interstellar medium, enriching galactic metal content, through the production of white dwarfs and supernovae. All the important processes involved are traced by the presence of hot (10^5–10^7 K) gas. High resolution spectroscopic observations at soft X-ray and Extreme Ultraviolet (EUV) wavelengths are essential to investigate the density, temperature, composition, magnetic field, structure, and dynamics of such plasma, addressing basic questions of stellar evolution and galactic structure.

The Scientific Objectives divide naturally into three broad categories, the study of Stellar Coronal emission, the local interstellar medium and white dwarfs and their companions. The science mission will comprise a combination of core and guest observer programmes. To illustrate the potential scope of the science in each area we provide an example target list (Table 1) that would occupy $\sim$1/2 of a nominal 3 year mission. We present below a more detailed description of each scientific theme.

2.1 Stellar coronae

The importance of studying magnetic activity on other stars goes beyond merely diagnosing stellar coronal plasmas and understanding their evolution with stellar age. The development of life on Earth has been influenced by the interplanetary environment around the Sun, which in turn is shaped by the magnetic properties of the Sun, i.e., its coronal EUV/X-ray flux, the particle flux in the solar wind, and frequent mass injections, all of which respond to the solar cycle. With SAGE, we propose a study of the coronae of a diverse and carefully selected sample of stars, comprising very young stars, main sequence stars, and more active systems with very high rotation rate. Our goal is to understand the physics that controls the evolution and characteristics of the hot corona and the resulting interplanetary environment.

With the advent of satellites, a wealth of new data exists not only for the Sun but for many chromospherically active stars such as M dwarfs, RS CVn binaries, etc. While the magnetic nature of atmospheric structuring and heating is uncontroversial, considerable uncertainty exists about the link between magnetic fields in the corona and interior of the Sun. How precisely the solar

Table 1 Example target list for the SAGE mission, indicating the science topics covered

Common name	Type	ks	WD objectives	Name	Spectral class	D (pc)	ks	Objectives
White dwarfs				Coronal sources				
GD2	DA	256	Trace metals	CPD-64 120	K1Ve	59	375	Young/Horolog assoc
RE J0029-632	DA	76	Trace metals	GSC8491-1194	M3Ve	40	355	Young/Horolog assoc
GD659	DA	136	He, trace metals	CD-53 544	K5Ve	40	266	Young/Horolog assoc
GD 50	DA	64	He, trace metals	TW Hya	K8V	56	338	Young/TW Hya assoc
RE J0457-281	DA	64	He, metals, stratification	CD-337795	M3V	50	281	Young/TW Hya assoc
RE J0503-285	DO	136	Non DA, abundances	HD 172555	A7	29	450	Young/Tucana assoc
G191-B2B	DAw	76	He, metals, stratification	HD 177171	F7	45	113	Young/Tucana assoc
GD 71	DAw	316	He, trace metals	HD 202917	G5	45	300	Young/Tucana assoc
RE J0623-374	DA	64	He, metals, stratification	HD 5578	K3/K4	44	240	Young/Tucana assoc
RE J0632-050	DA	200	Trace metals	β Ceti	K0III	29	160	Emission site
GD80	DAw	64	Int. temp DA, metals?	UX Ari	G5V/ K0IV	50	600	Doppler imag/flares
RE J0715-705	DA	100	Trace metals	V711 Tau	G5IV/ K1IV	29	440	Doppler imag/flares
RE J0723-274	DA	64	Int. temp DA	α Aur	G5IIIe + ?	13	160	Emission site
RE J1032+532	DA	88	He, trace metals	AB Dor	K1IV	15	720	Doppler imag/flares
LB 1919	DA	118	He, trace metals	σ Gem	K1III + ?	38	88	Emission site
PG 1123+189	DAw	136	He, metals, stratification	44 i Boo	G2V + G2V	12	224	Emission site
PG 1234+482	DA	124	He, metals, stratification	σ^2 Cor Bor	F6V/G0V	22	325	Doppler imag/flares
EG 187	DAw	250	He, trace metals	AR Lac	G2IV / K0IV	42	250	Emission site
H1504+65	DO	76	Non DA, abundances	λ And	G8V-IV + ?	26	88	Emiss site/flares
HZ 43	DAw	293	He, trace metals	EP Eri	K1V	5	160	Main sequence
BPM 93487	DA	100	He, trace metals	κ Cet	G5V	9	300	Main sequence
RE J2009-602	DA	94	He, trace metals	39 Tau	G5V	17	260	Main sequence
RE J2156-543	DA	106	Pure H DA	χ1 Ori	G0V	9	160	Main sequence
RE J2214-491	DA	64	Very hot DA/metals	α CMi	F5IV-V	4	50	Main sequence
GD 246	DAw	200	Hot DA/metals	β Com	F9.5V	9	310	Main sequence
RE J2324-547	DA	88	He, trace metals	HD 115404	K2V	11	250	Main sequence
RE J2334-471	DA	64	He, metals, stratification	α Cen	G2V + K1V	1	20	Main sequence

GD 984	DA+dM	256	He, metals, stratification	ξ Boo A (+ B)	G8V	7	160	Main sequence
SAO248569	DA	64	He, trace metals	36 Oph A	K0V	5	100	Main sequence
Feige 24	DA+dM	64	He, metals, stratification	70 Oph A	K0V	5	200	Main sequence
V471 Tau	WD+k0	148	DA+ dK binary, pre-CV	15 Sge	G1V	18	200	Main sequence
HR1608	DA+K	456	DA + K binary	61 Cyg A	K5V	3	170	Main sequence
HD33959C	DA+F	125	DA + F binary	CF Tuc	G0V / K4 IV	86	75	Flare studies
Sirius B	DA+AIV	76	Trace metals	UV Cet	M5.5Ve	5	75	Flare studies
RE J0718-312	DA+dM	128	Da + dM binary	YY Gem	dM1e/dM1e	1	75	Flare studies
RE J0723-318	DA+dM	240	Pre-CV	YZ CMi	M2Ve	7	75	Flare studies
GD394	DAw	173	Pre-CV	AD Leo	M4.5Ve	5	75	Flare studies
HR 8210	DA+A	125	He, trace metals	EK Dra	G1.5V	34	75	Flare studies
CPD -71 277	DA+G	76	He, metals, stratification	BY Dra	K4V / K7V	16	75	Flare studies
Cataclysmic variables and related objects				VW Cep	G8 / K0	23	75	Flare studies
SS Cyg	DN	240	Dwarf nova	AU Mic	M2Ve	9	75	Flare studies
U Gem	DN	240	Dwarf nova	FK Aqr	dM2e/dM3e	9	75	Flare studies
OY Car	DN	240	Dwarf nova	EV Lac	M4.5Ve	5	75	Flare studies
VW Hyi	DN	160	Dwarf nova	II Peg	K2IV/M0-3V	42	75	Flare studies
EX Hya	DQ	300	Intermediate Polar	ε Eri	K2V	3	90	Planetary system
HU Aqr	AM	160	Magnetic (Polar)	47 Uma	G1V	13	200	Planetary system
BL Hyi	AM	320	Magnetic (Polar)	51 Peg	G2.5IV	15	200	Planetary system
UZ For	AM	200	Magnetic (Polar)	Gleise 581	M3	6	100	Planetary system
AR Uma	AM	264	Magnetic (Polar)	Gleise 876	M4	5	100	Planetary system
EF Eri	AM	200	Magnetic (Polar)	Pollux	K0III	10	200	Planetary system
V834 Cen	AM	360	Magnetic (Polar)	υ And	F8V	14	200	Planetary system
AM Her	AM	360	Magnetic (Polar)	γ Cephei	K1IV	12	200	Planetary system
RR Tel	Nova	300	Symbiotic Nova	55 Cancri	G8V	13	200	Planetary system
RXJ05012.9-6951	SSS	300	Supersoft Source	Extragalactic				
Cal 83	SSS	300	Supersoft Source	PKS2155-304	AGN		300	Halo/IGM
AM Cvn	AM CVn	300	AM CVn	MKN 421	AGN		300	Halo/IGM
GP Com	AM CVn	300	AM CVn					

magnetic dynamo operates, how a magnetic dynamo was formed in the youth of the Sun, and how it changed as the Sun evolved, are unanswerable questions at the moment. From a comparison of the Sun with other stars, we know that it is quite inactive. Its typical coronal temperature is $\sim$1M K, reaching $\sim$5M K in active regions and $\sim$15M K in flares. Each of these features produces characteristic spectra. At 1–5M K, the strongest emission is found in the 150–350 Å region, which also provides the best density diagnostics. At or above 10M K, the bulk of the emission is in the X-rays, but the strongest spectral lines from Fe XVIII–XXIV are actually in the 90–270 Å spectral region, where also the best density diagnostics are to be found (cf. Mason et al. [9]).

ROSAT and EUVE X-ray and EUV measurements have shown that most late-type stars with outer convection zones, i.e., stars of spectral type F through M are highly variable and possess, even in quiescence, much hotter plasma compared to the (average) Sun. The plasma parameters appear to depend on convection zone conditions and stellar rotation rates. ROSAT had broad-band instruments, and EUVE's sensitivity did not allow accurate measurements of densities or chemical abundances, nor accurate measurements of 1 MK plasmas. XMM-Newton and *Chandra* have provided high-resolution grating spectra, which have given us excellent measurements of temperatures and chemical abundances of 4–12M K plasmas. Unfortunately, the best density diagnostics are limited to 2–4M K plasma (O VII and Ne IX triplets), and these instruments were rather insensitive to T $<$ 4M K emission (with the exception of a few lines, and some weak ones observed by *Chandra* LETG). In contrast, the SAGE spectral windows are rich in strong emission lines formed from the chromosphere-transition region up to 12M K. SAGE will provide for the first time detailed measurements of 0.5–12M K plasmas. Thanks to detailed scattering calculations (e.g. Iron Project and UK R_{max} collaborations) and their availability (cf. the CHIANTI atomic database [10]), we now have good atomic data that can provide accurate density measurements. Accuracy in measuring N_e in the 10^7 K plasma is important, as previous results based on EUVE have been questioned.

SAGE measurements will provide key information to understand the emission in stellar coronae at a wide variety of stellar ages and activity, relating this it to what is known about the solar corona. Target objects will include:

- Very Young Stars: identify the sources of high-energy in Classical T-Tauri stars. EUV spectra will distinguish between coronal emission and an accretion stream. Line widths for a rotating corona could exceed those for an accretion flow, which would show Doppler shifted emission and opacity effects if densities are high. Densities at high-T could be determined from EUV line ratios to distinguish between a diffuse corona and a dense accretion stream or shock.
- Main Sequence Stars: SAGE will examine coronal heating and the structure of the mid and upper transition region and the inner corona, using a sample of stars on/near the MS varying in spectral class between G0 and K5 and cover a range of rotation periods and Rossby numbers. At present,

the most likely candidates for coronal heating are magnetic reconnection and MHD (e.g. Alfvén) waves.

- Hot Coronal Plasma and flares in Active Stars: In many active stars, coronal temperatures and densities are higher than on the Sun. The high-T coronal material is magnetically confined [11], but in rapidly rotating stars it may be extended and suffer turbulent broadening. SAGE will have the resolving power and sensitivity to allow location of hot plasma in rapidly rotating systems using line profiles and Doppler shifts, and more accurate N_e measurements. SAGE capabilities will allow us to determine the flare evolution at all temperatures, to measure flow velocities, non-thermal line broadening, abundances, and, in the stronger flares, N_e. Density measurements are important because they provide an indication of the volume of the flaring plasma.
- Abundance Anomalies: Feldman and Laming [12] reviewed coronal abundances prior to the launches of*Chandra* and XMM-Newton. EUVE and ASCA showed that abundance anomalies are present in: α CMi (F5IV), ε Eri (K2), α Cen AB (G2V + K0V), ξ Boo A (G8V + K4V), ξ UMa [13–17]. However measurements were uncertain. *Chandra* and XMM-Newton have shown that stars have a large variation in their abundances, with many active stars having an inverse FIP effect. For example, Drake and Testa [18] and Sanz-Forcada et al. [19] derive large relative abundances of N_e in a number of stars. These large differences are puzzling. Testing of various models demands high sensitivity and spectral resolution, and SAGE offers increases by factors of ~50 over EUVE in the crucial 170–260 Å region, allowing more robust and sensitive detections of the FIP effect.

2.2 Stability of planetary atmospheres

In recent years we have seen an explosive discovery via radial velocity and transit programmes of extrasolar planets. The range of data to be obtained from the above studies has applications to this work. For example, to study the ways by which a star affects the chemistry and climate of a planet in its habitable zone, it is necessary to have spectra ranging from the X-ray to IR. However, much of the photochemistry in the planetary atmosphere is driven by the shorter wavelength photons and, therefore our knowledge of the EUV and UV spectrum is critical. Stellar variability is also an important issue as regards the atmospheric chemistry of a planet. On time scales of hours to years, many main sequence and dM stars exhibit extreme and intermittent variability due to the star's magnetic activity, e.g. flaring can produce a hundred-fold increase in the EUV and X-ray fluxes. Data obtained from stars in the core programme, in both the flaring and non-flaring states is a necessary input for the modeling [20, 21]. The example target list (Table 1) includes stars with known planetary systems covering a range of spectral types. An important comparison will be made between these systems and the general targets that cover the whole range of stellar activity and which are not (yet) known to have planetary companions.

2.3 Spectroscopy of B stars

While O and B stars are expected to have strong emission in the EUV, most objects are too distant and too absorbed by the interstellar medium to be detectable. Indeed, only ε and β CMa were detected in the initial EUV sky surveys. ε CMa is in fact the brightest EUV source in the sky, but most of the flux lies at wavelengths beyond the range of the SAGE instrument. However, there are significant emission lines from HeII and Fe IX/X/XI, which do fall within the SAGE bands and which could be used to study the physical properties of the gas in the hot winds of these stars.

2.4 White dwarfs, their companions and circumstellar material

White dwarf stars play a key role in many still open and important astronomical questions related to galaxy evolution and enrichment. Their space and luminosity distributions help map out the history of star formation in the Galaxy and can be used to determine the age of the disk. They have an intimate relationship with interstellar gas (ISM), a fundamental component of the Milky Way and other galaxies. The local interstellar medium (LISM) is close enough to us for detailed examination of its composition and structure, which tells us about the evolution of the Universe and our galaxy. Production of white dwarfs in the disk substantially enriches the content of the local ISM, contributing significantly to the total cosmic abundance of metals, particularly CNO (e.g. Barstow and Werner [22]), and these stars also make good background sources against which interstellar material can be detected. There is compelling evidence that some white dwarfs are surrounded by circumstellar material [23], which may be a remnant of earlier mass loss phases. However, the recent discovery that a number of cooler white dwarfs have debris disks (e.g. Kilic et al. [24]) is a strong indication that the stars may be accreting material from remnant planetary systems in form of asteroids or comets (e.g. Jura [25]). Since many stars are born in binary (or triple) systems, white dwarfs in binaries represent one of the most common products of binary evolution. These binaries are key objects to understand the mechanisms which drive the evolution of low mass binary systems as they are also believed to play a significant role in the production of the cosmologically important type Ia supernovae, through stellar mergers or mass transfer.

Internally, white dwarfs are also formally analogous to neutron stars, being stellar configurations where the thermal contribution to support is secondary. Both stellar types have various intrinsic and environmental parameters. Comparison of such analogous systems using scaled parameters can be fruitful [26]. Source class characterization is mature enough that such analogies can be used to compare theoretical ideas across a wide dynamic range in parameters, one example being theories of quasiperiodic oscillations. However, the white dwarf side of this program is limited by the available photometry and spectroscopy at EUV wavelengths, where there exist critical spectral features that contain diagnostic information often not available at other wavelengths. Moreover, interstellar absorption makes EUV observations challenging. Dynamical timescales and the envisioned performance of SAGE make possible a new level of source modeling. Sometimes wrongly dismissed for limitations of small bandwidth or local view from optical depth limitations, the EUV is instead a gold mine of information bearing upon key issues in compact objects, but it is information that must be won through the triple combination of high spectral resolution, large area, and application of advanced theory.

White dwarfs are among the oldest stars. Their distributions help map the history of star formation in the Galaxy and in principle help determine the age of the disk. Cool WDs may account for a fraction of the missing mass in the galactic halo [27]. To understand and calibrate cosmologically important aspects of WDs (such as their cooling ages, masses, and compositions) calls for thorough understanding of how their photospheric compositions evolve. Atmospheric metal abundances affect cooling rates and bias determinations of temperature and surface gravity. A reliable mass can be derived only from accurate effective temperature ($T_{\rm eff}$) and surface gravity (g). Metals are hard to detect in cool WDs but play an important role in cooling. Abundances in hotter stars tell what species may be present.

As end-products of the lives of all stars below ~8 $M_\odot$, representing >90% of the galactic stellar population, WDs reveal complicated and poorly understood processes during the rapid and complex phase of post-MS evolution. SAGE will conduct a systematic survey for photospheric helium in the DA WDs. Target selection will include isolated WDs and WDs with binary companions, covering a range of $T_{\rm eff}$ and g, and span a range of heavy element compositions. SAGE will map the abundance of He (when present) by $T_{\rm eff}$, g and heavy element composition and will study the effect of common envelope evolution and associated mass-loss. With typical S/N~20, SAGE will have a detection limit of He/H (by number) $\sim 5 \times 10^{-8}$, more than 2 orders of magnitude below that achievable with FUV observations (e.g. by Barstow et al. [28]). Low

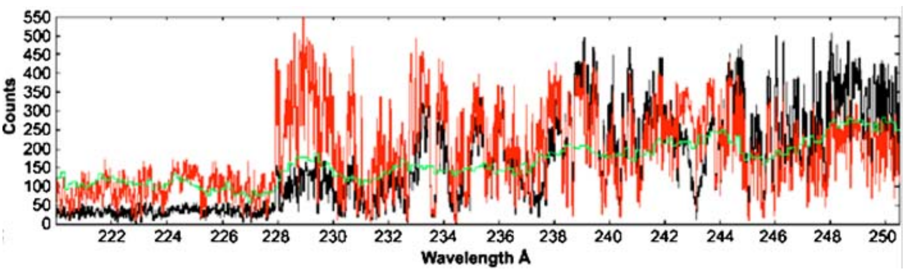

Fig. 2 Simulated 4,000 s exposure of the DA WD + dM binary Feige 24, for H layer masses of 10^{-13} (*red/grey*) and 10^{-14} (*black*) M$_/$. The *green histogram* shows an actual EUVE observation. Poission noise has been included in the simulation, but all fluctuations are "real" spectral features

levels of photospheric He will be detectable even when significant quantities of heavier elements are present (see Fig. 2).

High-resolution EUV spectra of heavy element-rich DA stars, only obtainable with SAGE, allow measurement of photospheric abundances and their depth dependence. Outcomes reflect several processes, including mass loss, radiative levitation, gravitational settling, and accretion from the LISM. An important control group will be DAs with apparently pure H envelopes, where improved sensitivity may allow detection of material at levels well below current limits, but which must be present if current theory is correct. Understanding heavy element transport in WD envelopes is critical to understanding how thermonuclear releases are initiated in classical novae; it is difficult to trigger novae without heavy elements being present.

Binary systems containing single or double degenerate white dwarf stars represent key systems to study the late evolution and properties of low-mass close-binary systems and include several subclasses of likely SNIa progenitors. The evolution of white dwarfs in close-binary systems can be profoundly altered by several mechanisms of mass exchange. The system may experience a common envelope phase while the WD progenitor is a red giant, leading to mixing of outer envelopes and possible mass expulsion. Later, the WD may accrete material, either at a low level by intercepting the stellar wind of its companion or as direct transfer through Roche lobe overflow. Among WD binary systems, the most numerous are the cataclysmic variables which consist of WDs accreting from Roche-lobe filling late type main sequence or, in rare cases, a giant companion. CVs offer a rich set of interesting physical processes, such as accretion disks in systems with non-magnetic white dwarfs, plasma interaction with high magnetic fields in those systems with magnetic white dwarfs, and eruptive or stable nuclear shell burning. All these processes produce large amounts of X-ray emission. The SAGE resolving power and effective area will permit detailed dynamical studies of the different high-energy processes. Magnetic CVs have magnetic moments ($\mu = 10^{30}$ to 10^{33} G cm^3) exceeding those found in any *accreting* NS. In classical novae CVs, accretion of H-rich material ($>\sim 10^{-4}$ $M_{\odot}$) leads to thermonuclear runaways on the WD surface and ejects processed material into the ISM. Novae may also enter a short lived (up to 10 years) super-soft X-ray phase which is still poorly understood but of key importance to elucidate the link between CVs and one of the progenitor channels of type Ia SNe. Double-degenerate ultracompact systems, the AM CVns, consisting of a WD accreting from a H-deficient degenerate companion have also been proposed as an alternative channel to type Ia SNe. The use of SNIa as standard candles on cosmological scales should be backed by better understanding of the progenitors.

2.5 The local interstellar medium

The ISM within 200 pc of the Sun can be probed by SAGE using bright EUV sources, seen with high resolution through different optical depths and gas cloud structures along various lines of sight. This EUV technique has yielded much in the past; SAGE will refine it, with broad astrophysical impact. FUSE, Chandra, and SAGE bring new levels of rigor and insight to ISM studies, with SAGE covering temperature and ionization states not accessible to the others. The local ISM, within ~200 pc of the Sun, is the only interstellar plasma in the universe accessible in this way. The limiting factor for detection of weak ISM lines is the S/N achievable for the instrument resolution and detector background. SAGE will obtain S/N 10–50, and we are exploring techniques to enhance this further.

Of all elements observed within the warm local clouds, He is most sensitive to non-equilibrium ionization conditions. The H ionization ratio, being extremely sensitive to the stellar EUV radiation field, reflects ionization equilibrium, but the He II/He I ionization ratio (because of the higher He I ionization potential $\chi_i = 26.6$ eV), is insensitive to the EUV radiation field. He ionization is a diagnostic of non-equilibrium ionization within the clouds and detection of interstellar He is possible only in the EUV. SAGE will obtain high-resolution spectra of the He II Lyman series of a sample of white dwarfs, including the He II ionization edge at 228 Å (e.g. Fig. 2) and the He I autoionization feature at 206 Å. The high spectral resolution and effective area of SAGE allow us for the first time to disentangle interstellar He II and photospheric absorption in stars with substantial heavy elements, whose lines would be otherwise blended with the interstellar He II. Detection limits of $\sim 10^{16}$ atoms cm^{-2} for both He I and He II will be achieved by even modest S/N (~10:1) spectra. Combining SAGE results with column densities of low ionized species through the local cloud complex (HST and FUSE) gives us the optimum dataset for testing if He is in an ionization recombination phase and when the ionization event(s) occurred. These data may also shed light on the actual source of this unusual ionization pattern which may be linked to the origin of the Local Bubble cavity.

2.6 SAGE observations of extragalactic sources

Due to the significant opacity of interstellar hydrogen gas to the passage of soft X-ray and EUV radiation, the vast majority of stellar targets available for study by SAGE lie within 200 pc of the Sun. However, an interstellar chimney of low H column density links the top and bottom of the Local Bubble cavity to the overlying galactic halo [29]. This provides a 30 degree diameter window at high galactic latitudes through which SAGE can view distant sources such as halo white dwarfs, QSOs and BL Lac objects. PKS 2155–304 and Mrk 421 are two bright extragalactic sources which were observed with EUVE. Such objects are variable in flux, but when in high states can be studied near 100 Å, since the attenuation of the flux by H and He in the galactic halo drops off dramatically shortward of 110 Å.

Besides the Galactic Halo, SAGE will also sample hot gas coincident with the low-redshift Ly-α and O VI absorbing systems. Outside the Local Group, Chandra has been limited by S/N and resolution and has yielded tentative results for $z = 0.297$ for H1821 + 643 (S/N ~8 and R ~500) in a 470 ks exposure by Mathur et al. [30]). Data at high S/N can also confirm possible EUVE detections of any highly ionized species of Ne, Mg, and Fe identified in the beamed continuum of the relativistic jets of PKS 2155–304 and Mrk 421 [31, 32].

3 Proposed SAGE payload instrument complement

3.1 Overview

The SAGE instrument [5, 6] is based on the flight-proven J-PEX normal incidence EUV spectrometer concept (see Fig. 3), which needs minimal further development for this mission and utilises a multilayer coated diffraction grating to yield high reflectivity. While these multi-layers achieve high efficiency, this is over a limited waveband. Therefore, to cover a broad spectral range we propose to build a suite of eight spectrometers, each having a different waveband and together optimized for the proposed science over the total wavelength range 90–275 Å. Figure 4 is an optical layout diagram showing the slitless design comprising a figured diffraction grating operating at near-normal incidence in a Wadsworth mount [33]. The basic design is simple, has small aberrations, and yields large collecting areas. Its original heritage is the Skylab S-082A spectrograph (resolving power 10,000), which produced focused monochromatic solar images at the wavelengths of prominent emission lines. However, high-resolution astrophysical spectroscopy requires high sensitivity. Therefore, SAGE will use large blazed ion-etched gratings, employs multilayer coatings to enhance efficiency, and records spectra with efficient focal plane detectors.

The SAGE instrument mechanical layout is shown in Fig. 5. Each spectrometer has a door, which makes a dust-and light-tight aperture seal. Light enters

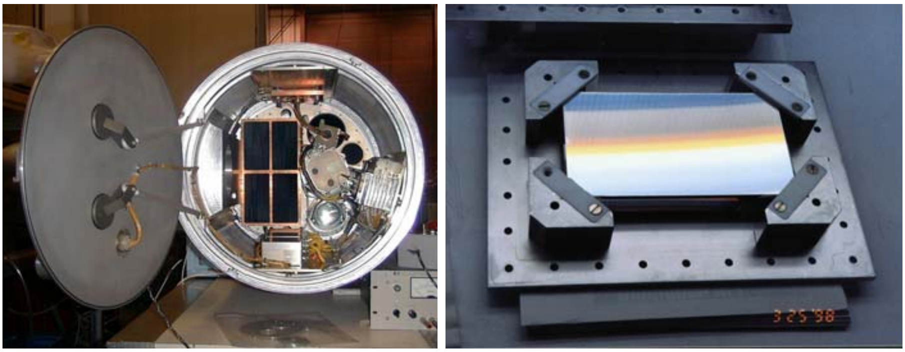

Fig. 3 *Left* Photograph of the aperture of the J-PEX spectrograph showing the collimators (*black rectangles*) and (*to the immediate left*) the MCP detector and associated electronics boxes. The two circular apertures are optical tracking telescopes. *Right* One of four segments of the J-PEX multi-layer coated grating

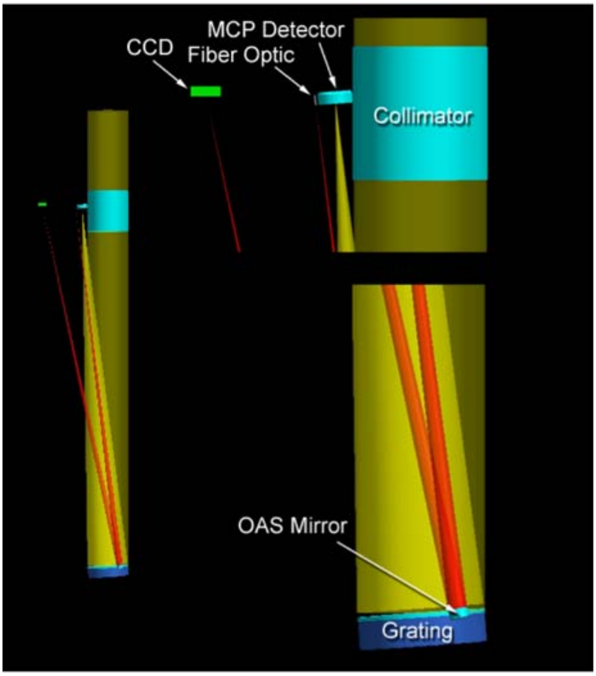

Fig. 4 Optical layout of a single SAGE spectrometer showing the off-axis arrangement of the MCP detector and the optical alignment and tracking CCD. The left hand schematic shows the full 3-m focal length while the right hand has a section removed to zoom in on the components

through a collimated aperture, which minimizes the flux of diffuse background radiation, and is diffracted by a grating to form a focused spectrum of a chosen order onto an MCP detector. All spectrometers are functionally identical, and the different wavebands are defined primarily by the multilayer coating.

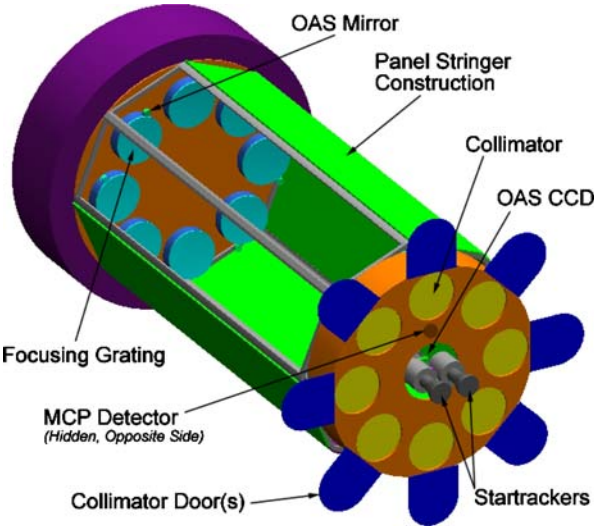

Fig. 5 Arrangement of the eight proposed spectrometers on board the SAGE spacecraft

Table 2 Detailed design of the multi-layers for each spectrometers waveband

Spectrometer	1	2	3	4	5	6	7	8
Grating Focal Length (mm)	3000	3000	3000	3000	3000	3000	3000	3000
Detector+Grating Aberrations (Microns)	25	25	25	25	25	25	25	25
Grooves/mm	3600	3600	3600	3600	2700	3600	3600	3000
Blaze Order	2	2	2	2	2	1	1	1
Angle of Incidence (Degrees)	4.05	4.46	4.83	5.45	5.42	4.13	4.65	4.27
Average Resolution (R)	8467	9331	10109	11405	11340	8640	9720	8928
Peak Wavelength (Angstroms)	98	108	117	132	175	200	225	248
Detector Active Size (mm)	50	50	50	50	50	50	50	50
Wavelength Range (Angstroms)	23.1	23.1	23.1	23.1	30.9	46.3	46.3	55.6
Lower Limit (Angstroms)	86.4	96.4	105.4	120.4	159.6	176.9	201.9	220.2
Upper Limit (Angstroms)	109.6	119.6	128.6	143.6	190.4	223.1	248.1	275.8
# Periods Multilayer (Nodal/Spacer)	30 Mo/Y	30 Mo/Y	17 Be/Mo4Ru6	12 Mo2C/Si	6 Mo2C/Si	9 Mo2C/Si	8 Mo2C/Si	7 Mo2C/Si
%Saturation – rms (Angstroms)	52.6–5	69.6–5	54.5–6	53.4	50.7	79.2	82.2	82.2
Multilayer Peak Reflectance	0.217	0.366	0.384	0.388	0.287	0.383	0.340	0.307
T_{Spacer} (Angstroms)	26.91	30.28	28.90	35.10	50.97	67.93	81.60	92.87
T_{Nodal} (Angstroms)	23.40	25.51	31.58	33.40	42.92	38.57	39.11	40.17
Detector QE or Material	0.55	0.50	0.50	0.45	0.40	0.30	0.30	0.30
Filter Transmission or Materials	0.66	0.63	0.60	0.55	0.55	0.52	0.47	0.42
Groove Efficiency	0.50	0.50	0.50	0.50	0.50	0.50	0.50	0.50
Collimator Transmission	0.90	0.90	0.90	0.90	0.90	0.90	0.90	0.90
Grating Diameter (cm)	35	35	35	35	35	35	35	35
Geometrical Area (cm^2)	962.1	962.1	962.1	962.1	962.1	962.1	962.1	962.1
Integral (Angstroms cm^2)	116.9	206.3	347.3	434.1	484.1	616.9	601.2	610.0

Wavelength Coverage >	10	cm^2 =	123.4	Angstroms	Σ Integrals (Angstroms cm^2)=		3416.7

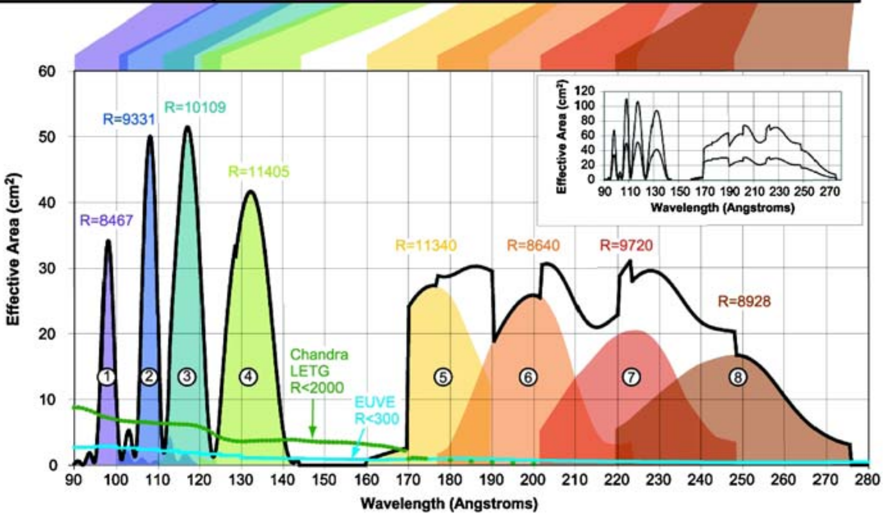

Fig. 6 Baseline effective area of SAGE (*inset*: baseline and best-case effective area sums)

Spectrometer characteristics (colour coded) and predicted performance (average resolution R and baseline effective area) are shown in Table 2 and Fig. 6, respectively. The thick black line is the summed effective area in regions where wavebands overlap. The effective area is the product of geometrical area, grating groove efficiency, multilayer reflectance, collimator transmission, filter transmittance, and detector quantum efficiency (QE), as explained in following sections. We have assumed conservative values for these quantities that are based on actual performance data. The inset to Fig. 6 shows a dramatic increase in effective area when the highest published values are used in the calculations, particularly for the best detector photocathode QE. However, all sensitivity calculations in this paper use the baseline effective area curve.

SAGE will achieve effective areas of at least 30–50 cm^2 at selected wavelengths and with coverage exceeding 10 cm^2 over ~67% of the range 90–275 Å. At the location of important spectral lines the SAGE baseline effective area exceeds that of Chandra and EUVE by an order of magnitude (Chandra LETG response extends to ~170 Å). The SAGE resolving power of ~10,000 exceeds that of Chandra by at least a factor of 5, and EUVE by a factor of ~30. This combination of simultaneous high effective area and resolution makes SAGE a powerful instrument.

A slitless spectrometer of high resolution has an advantage over competing designs (e.g., Rowland circle with slit, as in FUSE) in that it does not place tight requirements on the spacecraft (S/C) attitude control system (ACS). Modest pointing error, drift, and jitter may be tolerated provided these motions are calibrated out. The SAGE mission plans to use two star trackers, which together should produce precise (<1 arcsec) time-resolved pointing knowledge. This information will later be de-convolved from the time-tagged photon positions in the raw detector images to recover the designed spectral resolution. A sophisticated optical alignment system (OAS) with partial redundancy will monitor alignment and wavelength scale. The SAGE Central Electronics Unit (CEU), mounted in the S/C, will need to be equipped with a computer that controls the instrument and handles data, power, and command interfaces (I/Fs) with the S/C. The wavelength scale of the instrument will be provided initially by ground calibration using an emission line source and will be updated in orbit from measurements of emission lines from selected well-observed standards, as there is no suitable calibration source that can be carried on board the spacecraft.

3.2 Diffraction gratings and optical design

Holographic ion-etched gratings have very regular groove profiles and low surface micro-roughness (<5 Å) superior to that of ruled gratings as measured by atomic force microscopes (AFMs). These advantages in topography lead to higher efficiency. Grating groove efficiency is an evaluation of grating quality. It is most often derived from measurements, but can be predicted accurately using models of the groove profile, which may be theoretical or determined from AFM measurements. Excellent agreement between models and measurements of multilayer gratings is now routine. The maximum groove efficiency for an ideal laminar grating occurs in first order and is 40.5% [34]. The best J-PEX laminar grating had a groove efficiency of 34%, approaching the ideal limit, and with uniformity better than 10% (area 16 × 8 cm). We propose to use blazed gratings for SAGE as they offer two distinct advantages. First the groove efficiency of an ideal blazed grating can approach 100% in a chosen order [35]. Second, this performance may be achieved in higher grating orders, allowing achievable groove densities at short wavelengths or at high-resolution.

Until recently, the best blazed grating groove efficiency achieved was only 27%, but steady efforts at Carl Zeiss (Germany) have produced significant gains resulting in measured groove efficiencies of 40% in test gratings [36, 37] and 50% [38] in flight gratings that will be used in a new J-PEX mission. AFM-based models predict groove efficiencies in excess of 50% in second order and 66% in first order can eventually be achieved, but we conservatively assume 50% for groove efficiency (Table 2) in calculating effective area. Programmatic risk can be reduced by limiting the number of different groove densities that need to be manufactured. Tests show that grating resolution is unchanged with multilayer application, and a diffraction-limited resolving power (R) of 9,000–14,000 has been measured on sample gratings [39, 40]. Our 2-m focal length J-PEX flight spectrometer produced R$\sim$3,000. To achieve our target resolution, the SAGE gratings will have a longer, 3-m, focal length (1 arcsec -14.5 μm), a similar high groove density, and five of them will operate in second inside order. The groove densities (2,700–3,600 g/mm, Table 2) are comfortably within current technical limits, but the large grating diameter (35 cm) will require an upgrade of current manufacturing facilities.

Figured grating substrates may be made with high precision, so that aberrations are primarily geometric. Ray-tracing techniques, used to calculate grating aberrations for spherical and parabolic gratings with straight (parallel) grooves [41] and for spherical gratings with curved grooves [42] show a similar performance for the latter two cases. However, a spherical grating is much cheaper to produce than a parabolic one and has significantly smaller slope error. Thus, spherical gratings with curved grooves have been chosen for the SAGE baseline design. The final spectral resolution may be calculated from the rms sum of grating aberrations, the detector blur circle, pointing knowledge uncertainty, and collimator diffraction. The last three terms are relatively insensitive to wavelength (values discussed in later sections). From ray-tracing, the average value of grating aberrations over the waveband is 13 μm for all spectrometers. The calculated rms sum is 25 μm, producing the average value of R shown in Table 2. However, R also varies over each waveband, e.g., spectrometer 4: from 12,400 at the multilayer peak to 9,830 in the wings.

3.3 Multilayers

Multilayers consist of alternating thin layers of high- and low-absorption materials and are used to enhance the reflectivity of the normal incidence optics. Incident light near the design wavelength is reflected and transmitted by each bi-layer, and layer thickness is designed to produce constructive addition of reflected components so that multilayers function like synthetic Bragg crystals. For any given design layer structure the reflectance can be predicted theoretically and so the layer thicknesses can be optimised to maximise the efficiency. Real multilayers regularly achieve the predicted performance. Each SAGE spectrometer design (Table 2) has been optimized in an iterative process to cover selected spectral lines important for achieving our science goals. Peak reflectance increases with the number of bilayers (N_P), while bandwidth decreases. For SAGE, N_P has been chosen to provide a balance between peak reflectance and bandwidth. This provides a high degree of programmatic margin as N_P can be optimized shortly before deposition in response to the measured performance of other spectrometer subsystems. The choice of the layer materials also has an impact on reflectivity. There are prospects that new combinations may yield even better performance and the baselines options listed in Table 2 will be re-evaluated during the study phases of the mission. Multilayer reflectance is also affected adversely by layer roughness and material inter-diffusion. These are more significant at shorter wavelengths, so calculations for the three shortest SAGE wavebands include a Debye–Waller factor. Long-term multilayer stability has been investigated as well, and there is no significant loss in performance over many years provided that surfaces are kept clean of contaminants, particularly hydrocarbons [43, 44].

3.4 Focal plane detectors

The detector of choice for EUV instruments has in the past been a photon counting microchannel plate (MCP) stack with associated event position encoding electronics. The general goal is always to obtain the highest possible QE but SAGE places additional demands on spatial resolution to achieve the high spectral resolution goals. A readout design developed by the University of Leicester and Mullard Space Science Laboratory makes use of the "Vernier" anode. This employs a repeated sequence of nine linear anodes deposited on a multilayered substrate. The area of each anode varies along its length in a cyclic manner. Analysis of the charge collected by the anodes yields a 2-D image. The Vernier anode produces non-linearities <20 μm rms with spatial resolution limited only by MCP pore size. This mechanical design is based on the ROSAT WFC, and a prototype detector employing the Vernier anode and 10 μm pore MCPs was flown successfully on the J-PEX mission. For SAGE we will use an improved version of this detector utilising 6 μm pore MCPs. In a standard "chevron" MCP pair configuration we have already demonstrated that we can achieve the desired gain uniformity, pulse height distribution, low background rate (0.2 cnts cm^{-2} s^{-1}), flat field uniformity, and high QE [45, 46].

In the EUV detectors have to be "open face", as there is no suitable window material that allows high transmission yet can retain a vacuum seal. High quantum efficiency requires use of an alkali halide (e.g., CsI, CsBr, KBr) opaque photocathodes deposited on the MCP surface optimized for 100–300 Å. These materials are highly sensitive to contamination and will degrade to varying degrees in the presence of water vapour. Therefore, each detector unit will need to be protected by an open-able door during ground testing and launch. We already have a proven design flown on J-PEX.

One disadvantage of MCP detectors is the limited quantum efficiency (∼20–30%) achievable with even the best photocathodes. In other wavelength ranges CCD detectors have become ever more efficient, approaching 100%

at some wavelengths, but until recently EUV efficiencies were always very low. However, back-thinned CCDs have been developed for the EIS EUV spectrograph flown on board the JAXA solar mission Hinode. These devices were produced by e2v and have a 2,048 × 1,024 pixel format and 13.5 μm pixel size, which is compatible with the needs of the SAGE spectrographs, and have a quantum efficiency of 40% across the wavelength range of interest [47]. However, CCDs have some disadvantages in the SAGE context when compared to MCP detectors. They need cooling (to ∼ −50°C) and the frame readout time (0.8 s) limits the temporal resolution of the instrument. While no sources are sufficiently bright for a spectrum to be accumulated on this timescale, it may be an issue for attitude reconstruction and achieving the target resolution. The trade-off between MCP and CCD detectors will need to be studied in the future.

3.5 Collimators

To minimize UV background flux, each spectrometer aperture will be equipped with a high transmission honeycomb collimator (FOV 1.25°). Techniques for assembling accurate collimators from thin copper sheet, used successfully on J-PEX [48], will be adapted to SAGE. Collimator diffraction will be ∼5 μm at 98 Å and ∼10 μm at 225 Å. Collimator walls can be coated with Ebonol-C to inhibit multiple reflection of back-ground UV. Outgassing by Ebonol-C and the collimator bonding-adhesive has been examined, and will not be a significant contamination in the instrument.

3.6 Filters

The UV background scattered by the gratings and internal structure will be reduced to acceptable levels by a thin-film filter in each MCP detector. Two filter designs have been produced for SAGE. The first is a 600 Å polyimide film with a 200 Å Boron coating, which will be used for the four shortest wavelength spectrometers. The second is a 1,200 Å aluminium film with a 200 Å graphite coating, for the longer wavelength spectrometers. The load-bearing substrates are the polyimide and aluminium. The filters will be supported by a mesh (transmission 82%) and launched under vacuum to avoid acoustic loads. However, the polyimide/Boron filter could be self-supporting, leading to a 22% increase in effective area. For simplicity, we calculated for each spectrometer one average transmittance (including mesh) at the peak multilayer wavelength (Table 2), except for that covering the 175 Å waveband, which includes the cut-off caused by the Al L-edge (∼170 Å).

3.7 Background

Detector background has three main causes: the intrinsic MCP background (or electron noise for a CCD), cosmic rays, and the diffuse UV background. The intrinsic background is 0.2 cts cm^{-2} s^{-1}, and ROSAT HRI experience indicates that cosmic rays should contribute 0.82 cts cm^{-2} s^{-1}. We have examined all sources of UV background (Drake, J.J., 1997, private communication) [49]. The strongest are lines of OI (1,304/1,356 Å), HI (1,215.7 Å), OII (833.8 Å), HeI (584.3 Å), HeII (303.8 Å), and OII (303.7 Å) produced by geocoronal and interplanetary scattering of solar radiation. The gratings diffract most of this background radiation into strategically located light traps. The detector records residual scattered light. The dominant source is H I (1,215.7 Å) radiation, whose intensity varies from 3,500 R (Rayleighs) on the night side to 35,000 R in daylight. SAGE expected background rates vary between 1.1–1.8 cts cm^{-2} s^{-1} night to dayside for the long wavelength spectrometers and 1.5–5.7 cts cm^{-2} s^{-1} for spectrometers 1, 2, and 4. The worst case is spectrometer 3 with a rate of 2.3–14.1 cts cm^{-2} s^{-1}.

4 Spacecraft requirements

The SAGE payload is an array of co-aligned EUV telescopes designed to point at individual astronomical targets. Consequently it needs to be accommodated on a three-axis stabilized spacecraft which provides the necessary subsystems to support operations in Low Earth Orbit. However, the mission places modest requirements on the capability of the spacecraft which enables re-use of already developed systems at relatively low cost to the project. The most demanding need is the stability of the spacecraft attitude once a target has been acquired (pointing accuracy 60 arcsec, stability 1arcesc/s) and the subsequent accuracy of the attitude reconstruction (1 arcsec), to ensure that the target spectral resolution is achieved. Spacecraft performance below these specifications will lead to a degradation of the instrument performance.

One possible launcher is the Vega vehicle, which can place 2,300 kg into LEO at an inclination of 5.2°. This orbit will ensure low background radiation. A preliminary analysis suggests that the Vega launcher and Kourou ground station will meet our operational needs, provided the Vega fairing can accommodate the 5.5 m long × 1.6 m diameter cylindrical envelope filled by our payload. The basic spacecraft requirements are summarised in Table 3.

Table 3 Spacecraft parameters/requirements for the SAGE mission

Parameter	Requirement	Parameter	Requirement
Payload mass	600 kg	Payload power	400 W
Spacecraft mass	600 kg	Spacecraft power	200 W
Total mass	1,200 kg	Total power	600 W
Payload (satellite) envelope	3.5 m (5.5 m) high x 1.5 m diameter	Science data rate Science data storage	65 kbps (max.) 1.2 Gb/day
Slew capability (180°)	< 9 min	Data downlink	1 contact/day
Pointing control 1 σ	60 arcsec	Orbit inclination	5.0 degrees (minimum)
Pointing knowledge 1 σ	1 arcsec	Orbit altitude	500 ± 50 km
Stability 3 σ	1 arcsec/sec	Mission lifetime	3 years (Ps = 0.85)
Ephemeris knowledge	< 10 km	Radiation environment	2 krad

5 Attitude control

The spacecraft must provide three-axis stabilisation and pointing within the requirements of the SAGE mission, to within 1 arcmin and a stability of 1 arcsec/s. Time tagging the received photons improves science performance with data processing on the ground. Acquisition of astronomical targets will require the spacecraft star trackers to be aligned with the payload optical axis. There will be no strong need for rapid pointing of the instrument apart from the desire to maximise observational efficiency. In LEO, many targets will be occulted by the Earth for part of the orbit, apart from those near the ecliptic poles. A slew capability of 20° in less than 60 s allows the possibility of observing at least two targets within a single orbit to allow full use of the available time. The star trackers should be mounted to the instrument assembly to minimize thermal distortions. Standard operational modes should provide inertial pointing, safe modes, autonomous momentum management, hierarchical fault tolerance and protection, and instrument bore-sight Sun avoidance.

6 Conclusion

We have described the proposed high resolution soft X-ray and EUV spectroscopy mission to carry out a survey of Stellar and Galactic Environments (SAGE). The payload is based on novel diffraction grating technology which has already been proven in a sub-orbital space mission and which is ready to fly on a satellite platform with minimal development. Consequently, with an appropriate platform and launch vehicle, we expect this to provide a low cost mission opportunity with enormous potential of simultaneous high resolving power (~10,000) and effective area (30–50 cm^2) in the wavelength range ~90–275 Å. This will allow application of the range of plasma diagnostic techniques that has already been used successfully in solar research, from satellites such as SOHO and the recently launched Hinode. This mission will yield a capability of studying the dynamics of the integrated light from other stars at the level of detail available for the Sun. At 124 Å SAGE will deliver an effective area eight times that of the Chandra LETG and more than five times the spectral resolution, producing a step-change in high-resolution spectroscopy of hot plasmas. SAGE will allow unambiguous detection and measurement of weak emission lines and absorption features, and enable the study of source structure and dynamics through measurement of line profiles and Doppler shifts.

Acknowledgements Work at NRL was supported by the Office of Naval Research under W.U. 3641: Application of Multilayer Coated Optics to Remote Sensing, by the NRL Bid and Proposal Job Number 76-6039, by NASA-Defense Purchase Request S-47440F: A Study of the Physics and Composition of White Dwarf Atmospheres using High Resolution EUV Spectroscopy, and by NASA-Defense Purchase Request W-19,881: Liquid-Overcoated Blazed Gratings. The authors thank D. Yentis, G. Fritz, D. Woods, and G. Clifford for their participation in J-PEX. M.A. Barstow acknowledges the support of PPARC and STFC.

References

1. Barstow, M.A., Holberg, J.B.: Extreme Ultraviolet Astronomy. Cambridge University Press, Cambridge (2003)
2. Kowalski, M.P., Wood, K.S.: The future of EUV astronomy. In: Strickman, L., Yentis, D., Kowalski, M. (eds.) NRL. Washington, DC NRL Memorandum Report 7650-04-0905, 2005, on CD (2003)
3. Cruddace, R.G., et al.: ApJ. Lett. 565, L47 (2002)
4. Barstow, M.A., et al.: Mon. Not. R. Astron. Soc. **362**, 1273 (2005)
5. Kowalski, M.P., et al.: SPIE Proc. **5164**, 1 (2003)
6. Kowalski, M.P., et al.: SPIE Proc. **5168**, 21 (2003)
7. Florinsky, V., Zank, G.P.: Galactic cosmic ray intensities in response to interstellar environments. In: Frisch, P.C. (ed) Solar Journey. ASSL, vol. 338, p. 281 (2006)
8. Kirkby, J., Carslaw, K.S.: Variations of galactic cosmic rays and the Earth's climate. In: Frisch, P.C. (ed) Solar Journey. ASSL, vol. 338, p. 281 (2006)
9. Mason, H.E., Bhatia, A.K., Neupert, W.M., Swartz, M., Kastner, S.O.: Sol. Phys. **92**, 199 (1984)
10. Landi, E., Del Zanna, G., Young, P.R.: Astrophys. J. Suppl Ser **162**, 261 (2006)
11. Young, P.R., et al.: Astrophys. J. **555**, L121 (2001)
12. Feldman, U., Laming, J.M.: Phys. Scripta. **61**, 222 (2000)
13. Drake, J.J., et al.: Astrophys. J. **443**, 393 (1995)
14. Laming, J.M., Drake, J.J., Widing, K.G.: Astrophys. J. **443**, 416 (1995)
15. Laming, J.M., Drake, J.J., Widing, K.G.: Astrophys. J. **462**, 948 (1996)
16. Laming, J.M., Drake, J.J.: Astrophys. J. **516**, 324 (1999)
17. Ball, B., et al.: Astrophys. J. **634**, 1336 (2005)
18. Drake, J.J., Testa, P.: Nature **436**, 525 (2005)
19. Sanz-Forcada, J., et al.: Astron Astrophys **416**, 281 (2004)
20. Heath, M.J., et al.: Orig. Life Evol. Biosph **29**, 405, (1999)
21. Segura, A., et al.: Astrobiology **3**(4), 689 (1999)
22. Barstow, M.A., Werner, K.: Astrophys. Space Sci. **303**, 3 (2006)
23. Bannister, N.P., et al.: Mon. Not. R. Astron. Soc. **341**, 477 (2003)
24. Kilic, M., et al.: Astrophys. J. **646**, 474 (2006)
25. Jura, M.: Astrophys. J. **653**, 613 (2006)
26. Wood, K.S., Kowalski, M.P., Cruddace, R.G., Barstow, M.A.: J. Adv. Spa. Res. **38**, 1501 (2006)
27. Oppenheimer, B., et al.: Science **282**, 698 (2002)
28. Barstow, M.A., et al.: Mon. Not. R. Astron. Soc. **325**, 1149 (2001)
29. Welsh, B.Y., et al.: Astron Astrophys **352**, 308 (1999)
30. Mathur, S., Weinberg, D.H., Chen, X.: Astrophys. J. **582**, 82 (2003)
31. Cagnoni, F.: Astrophys. J. **546**, 877 (2001)
32. Königl, A., et al.: Astrophys. J. **446**, 598 (1995)
33. Feldman, U., et al.: Astrophys. J. Suppl. **81**, 387 (1992)
34. Hellwege, K.H.: Z. Phys. **106**, 588 (1937)
35. Vidal, B., Vincent, P., Dhez, P., Neviere, M.: Proc. SPIE. **563**, 142 (1985)
36. Kowalski, M.P., et al.: SPIE Proc. **5488**, 910 (2004)
37. Kowalski, M.P., et al.: Opt. Let. **29**, 2914 (2004)
38. Kowalski, M.P., et al.: 2006 SPIE proc., **6266**, 62660W1 (2004)
39. Kowalski, M.P., et al.: Appl. Opt. **32**, 2422 (1993)
40. Seely, J.F., et al.: Appl. Opt. **32**, 4890 (1993)
41. Hunter, W.R., Kowalski, M.P., Cruddace, R.G.: Appl. Opt. **42**, 6245 (2003)
42. Heidemann, K.F. Zeiss TG03-056 (2003)
43. Barbee, T.W. Jr., et al.: Appl. Opt. **32**, 4852 (1993)
44. Kowalski, M.P., et al.: Appl. Opt. **34**, 7338 (1995)
45. Bannister, N.P., et al.: Proc. SPIE **4140**, 199 (2000)
46. Lapington, J.S., Sanderson, B.S.: Proc. SPIE **4139**, 242 (2000)
47. Culhane, J.L., et al.: Solar Phys. **243**, 19 (2007)
48. Golembiewski, C.M., Cruddace, R.G., Kowalski, M.P.: Proc. SPIE **3445**, 197 (1998)
49. Meier, R.R.: Spa. Sci. Rev. **58**, 1 (1991)